Evaluating Performance of Two Group Interfacial Area Transport Equation for Large Diameter Pipes

A. Dave, A. Manera
Department of Nuclear Engineering and Radiological Sciences
University of Michigan
Ann Arbor, MI 48105, USA
akshayjd@umich.edu

M. Beyer, D. Lucas
Helmholtz-Zentrum Dresden-Rossendorf
Institute of Fluid Dynamics
01314 Dresden, Germany

ABSTRACT

In the two-fluid transport model, the coupling of mass, momentum and energy transfer between phases is highly dependent on interfacial area transfer terms. Several research efforts in the past have been focused on the development of an interfacial area transport equation model (IATE), in an attempt to eliminate the drawbacks of static flow regime maps currently used in best-estimate thermal-hydraulic system codes. The IATE attempts to model the dynamics that are involved in two phase flows by accounting for the different interaction mechanisms affecting bubble transport in the flow.

The further development and validation of IATE models has been hindered by the lack of adequate experimental data, especially in regions beyond the bubbly flow regime for large diameter pipes. At the Helmoltz Zentrum Dresden Rossendorf (HZDR) experiments utilizing wire mesh sensors have been performed over all flow regimes, establishing a database of high-resolution (in space and time) data [1]. A 195 mm diameter pipe with a 64 by 64 wire mesh sensor is utilized in the air-water experimental database used in this work. Analysis of flow conditions in the bubbly flow and churn-turbulent flow regimes is presented.

The performance of the current two-group IATE model is evaluated. While the qualitative propagation of interfacial area is predicted sufficiently well, there is a discrepancy in magnitude between the model's prediction and the experimental results. Overall, the study suggests that differences exist in the incidence of interaction mechanisms between small and large diameter pipes and further efforts are needed in order to extend the range of validity of current IATE models.

KEYWORDS
Two-phase flow, interfacial area transport, wire mesh sensor, large diameter pipe

1. INTRODUCTION

The two-fluid transport model is widely used in state of the art thermal-hydraulic system codes. A complete description of two phase flow is achieved through the two fluid model, which models the gas and liquid phase separately. There are three transport equations for each phase, resulting in six transport equations. The two fluid model is more accurate for transients where flow conditions are rapidly changing

and non-equilibrium field values exist for the phases. For example, the time lag of energy transfer at the interface may cause temperature difference between the gas and liquid phase. However, several closure relationships are needed for the interfacial transfer terms which couple the transport equations. As described by Ishii and Kim [2], these terms can be expressed by Eq. (1).

$$(Interfacial\ Transfer\ Term) \propto a_i \cdot (Driving\ Force) \quad (1)$$

In Eq. (1), a_i represents the interfacial area concentration. Thus, as the interfacial transfer terms couple the two phases, the importance of being able to correctly predict interfacial area concentration is apparent. Since the one-group and two-group interfacial area transport equation (IATE) was derived by Ishii and Kim [2], several experimental efforts have focused on validation.

Recent efforts have involved the use of conductivity probes in various two-phase flow test facilities. The 1-group IATE model was benchmarked against two-phase flow data for a small diameter pipe by Talley [3]. It was found that the for a small diameter pipe (5.0 cm), the 1-group model had lackluster performance for bubbly flow – the most rudimentary flow regime. The study also stated that further experiments involving large diameter pipes were necessary.

Another study by Bernard et al. [4] employs the two-group IATE model in TRACE as an alternative to the static-regime flow map approach. The study finds that implementing the two-group IATE model decreases error in interfacial area concentration prediction from ±42% to ±19%, for experiments with a small diameter pipe (4.83 cm). The study concluded that "additional database containing data near slug to churn-turbulent transition and fully churn-turbulent two-phase flow conditions will be invaluable". A primary reason for this conclusion is due to constrained capability of the conductivity probe. The uncertainty associated to measurements of the interface orientation (and thus interfacial area concentration) using conductivity probes can be rather high in churn-turbulent and annular flow regimes as the majority of the interface would be parallel to the probe.

A study by Smith et al. [5] used the two-group IATE model for large diameter pipe (15.2 cm) experiments using the conductivity probe. The results indicated poor performance of the two-group IATE model, with some errors as large as 50%. Similar to the previous studies mentioned, Smith et al. also concluded that additional experimental database for large pipes was necessary. To address these short comings, a mechanistic model was proposed specifically for large diameter pipes by Smith et al. [6]. While the model was successful for pipes $D < 0.10\ m$, greater than 15% error was realized for $D > 0.10\ m$ at void fractions greater than 0.3.

The objective of this study is to assess IATE performance against a high resolution experimental database that covers a wide range of two-phase flow regimes. The experimental database is obtained from the TOPFLOW facility at Helmholtz-Zentrum Dresden-Rossendorf [1]. The TOPFLOW facility has a vertical 8 m long, 195 mm diameter, test section that has a fixed position wire mesh sensor. The wire mesh sensor enables void fraction distributions to be captured at a high resolution and high frequency (TOPFLOW is fitted with a 64 by 64 array with a bi-directionally equidistant spacing of 3 mm that is operated at a frequency of 2.5 kHz).

The void fraction measurement capabilities of the wire mesh sensor have been compared to ultra-fast X-ray tomograph by Prasser et al. [7]. The study indicated good agreement between the two instruments and lauded higher resolution (in time and space) capabilities of the wire mesh sensor. Furthermore, the performance of the wire mesh sensor versus the conductivity probe was studied by Manera et al. [8]. The interfacial area detected for viable flow regimes had good agreement. However, the wire mesh sensor provides several benefits. Since the data is acquired at a high spatial resolution, the duration of the experiments is significantly reduced (approximately 10 seconds of measuring for a test point versus

several hours for the conductivity probe). There are qualitative benefits that the wire mesh sensor provides – the acquired data provides a full reconstruction of the experiment allowing 3D visualization. Furthermore, the ability to gather accurate two-phase flow data in any flow regime is invaluable. The next section introduces relevant information regarding the experimental setup of the TOPFLOW facility and usage of the two-group IATE model.

2. BACKGROUND

A visual of the 8 m test section is provided on the left hand side of Figure 1. There are five major injection hubs that are located at exponentially increasing distances from the wire-mesh sensor. Each hub consists of three discs of radially isometric orifices. There are two discs that have 1 mm injection orifices (located at the top and bottom of each major hub). There is one disc that has 4 mm injection orifices (located in the middle of each hub). Each disc is able to operate individually or in conjunction with others. The rate at which water and air are injected are varied in order to achieve different flow regimes. The absolute pressure at the air injection is set at 0.25 MPa for each test point. As the pressure of air injected remains constant, but the injection location varies axially – the stationary wire-mesh sensor essentially records the axial development of two-phase flow over 8 m. The right hand side of Figure 1 displays the various tests conducted and are color coded to indicate flow regimes observed.

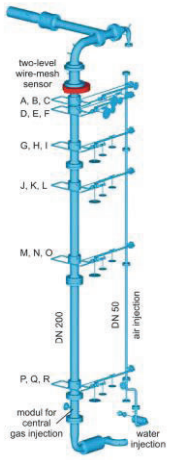

Superficial gas velocity J_G [m/s]

Superficial water velocity J_L [m/s]	0.0025	0.0040	0.0062	0.0096	0.0151	0.0235	0.0368	0.0574	0.0898	0.140	0.219	0.342	0.534	0.835	1.305	2.038	3.185	4.975	7.772	12.14	18.97
4.047	011	022	033	044	055	066	077	088	099	110	121	132	143	154	165	176	187	198	209	220	231
2.554	010	021	032	043	054	065	076	087	098	109	120	131	142	153	164	175	186	197	208	219	230
1.611	009	020	031	042	053	064	075	086	097	108	119	130	141	152	163	174	185	196	207	218	229
1.017	008	019	030	041	052	063	074	085	096	107	118	129	140	151	162	173	184	195	206	217	228
0.641	007	018	029	040	051	062	073	084	095	106	117	128	139	150	161	172	183	194	205	216	227
0.405	006	017	028	039	050	061	072	083	094	105	116	127	138	149	160	171	182	193	204	215	226
0.255	005	016	027	038	049	060	071	082	093	104	115	126	137	148	159	170	181	192	203	214	225
0.161	004	015	026	037	048	059	070	081	092	103	114	125	136	147	158	169	180	191	202	213	224
0.102	003	014	025	036	047	058	069	080	091	102	113	124	135	146	157	168	179	190	201	212	223
0.0641	002	013	024	035	046	057	068	079	090	101	112	123	134	145	156	167	178	189	200	211	222
0.0405	001	012	023	034	045	056	067	078	089	100	111	122	133	144	155	166	177	188	199	210	221

bubbly flow churn-turbulent flow annular flow

Figure 1: Schematic of the large diameter pipe used in TOPFLOW with indications of several injection points and location of the wire-mesh sensor (left) and experimental test matrix (right) [1].

2.1 IATE Interaction Mechanisms

In Section 3, the computational results are generated from TRACE-T (a developmental version of TRACE v5.0 p3 [3]). The two-group IATE model is implemented in TRACE-T. The two-group model was pioneered by Ishii and Kim [1] and focuses on separating spherical and non-spherical bubble shapes. The idea stems from the fact that there are significant differences in bubble interaction mechanisms and drag coefficients depending on the shapes of bubbles. While the one-group IATE model considers spherical bubbles only and is therefore is constrained to bubbly flows, the two-group model is meant for a broader range of flow regimes. The two-group formulation accounts for spherical and non-spherical bubbles by taking into consideration differences in bubble interactions and drag coefficients for each of the two groups. Figure 2 presents the equations for the two-group model. The left hand side of the

equation accounts for temporal and convective interfacial area (a_i) changes. The right hand side of the equation accounts for bubble volume changes (due to pressure drop) and the source and sink terms due to various interaction mechanisms (ϕ). Other variables and constants are detailed in the nomenclature.

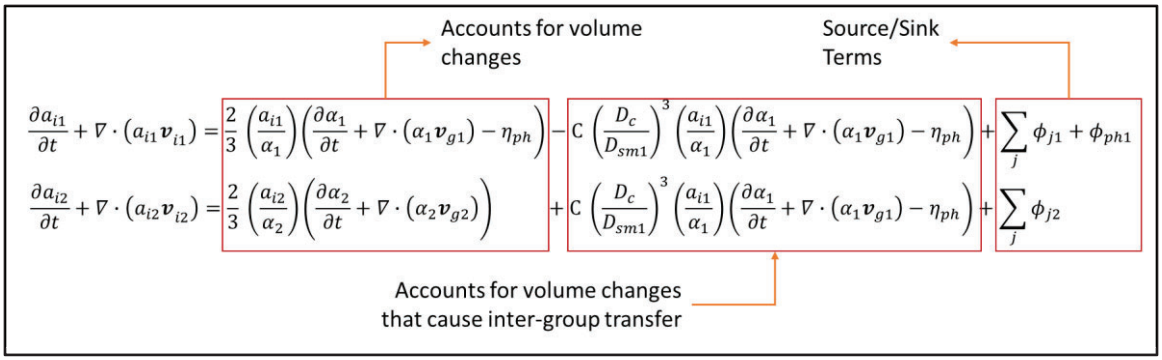

Figure 2: Two-group IATE model.

Figure 3 illustrates the various interaction mechanisms that are taken into consideration in two-group IATE. It is important to highlight that in the two-group IATE model, each separate interaction has a coefficient of proportionality (e.g. the random collision mechanism will require four coefficients). The coefficients are obtained empirically. Previous studies [9] determined these coefficients using experiments with smaller diameter pipes (about 50 mm). As indicated in the more recent studies cited in Section 1, validation of two-group IATE models for large diameter pipes has been hindered by a lack of experimental data.

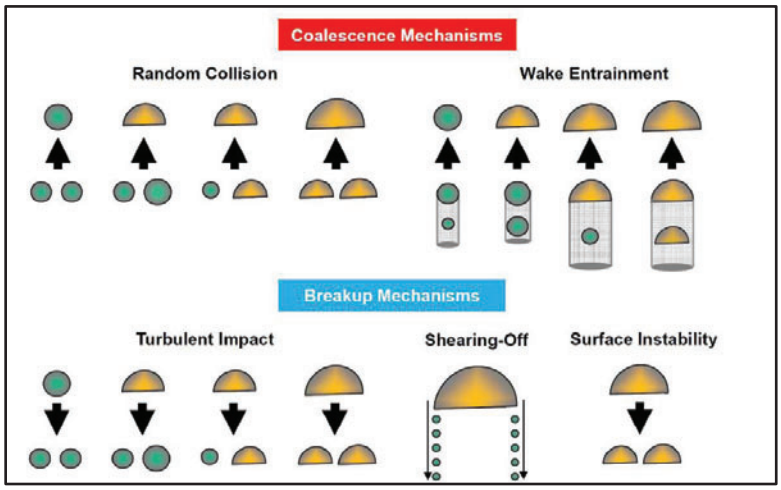

Figure 3: Interaction mechanisms modeled in two-group IATE. Green color indicates a group 1 bubble and yellow color indicates a group 2 bubble [10].

Detailed explanation for each mechanism can be found in [10]. Various formulations of the mechanisms and recommended values for the model coefficients exist; the model developed by Fu and Ishii [11] is used for the TRACE-T results presented in this paper. Although the Fu and Ishii model was not specifically developed for large diameters pipe, this model is deemed sufficient for the present analyses to highlight the role of the different break-up and coalescence mechanisms on the prediction of the

interfacial area density, especially in view of the fact that recent efforts on extending the models for pipe diameters larger than 10 cm have not yet been successful [6].

Two mechanisms that are prevalent in the results presented are briefly highlighted: wake entrainment and shearing-off. The wake entrainment mechanism occurs when a bubble enters the wake region of a leading bubble. The trailing bubble may accelerate and collide with the leading bubble resulting in coalescence. The collision frequency due to the wake entrainment mechanism is calculated by considering the density of bubbles in the wake region of the leading bubble. Shearing-off is a complex mechanism that arises for large bubbles. It is one of the least understood mechanisms. It occurs for large bubbles that form a skirt at the base of the bubble. The phenomenon is thought to occur because of disruptive viscous forces pulling at the rim of the skirt, overwhelming the local cohesive surface tension.

A closer look at the regimes observed in Figure 1 indicates that the slug flow regime, found in vertical two-phase pipe flow, is omitted. The reason for this omission is due to the fact that slug flow regime does not exist in larger test section diameter, with bubbly/cap flow transiting directly to churn flow regime. Prasser et al. [12] studied the differences in void fraction and bubble size distributions between a 51.2 mm and 194.1 mm diameter pipe, presented in Figure 4. In a small diameter pipe, the onset of slug flow is realized by a second peak in the bubble size distribution. In larger diameter pipes, this peak is less pronounced and wider. With accompanying qualitative observations, the slug flow regime was no longer present as the flow transitioned directly from bubbly to churn turbulent flow. This phenomena was explained by suggesting that the decreased confining action of the wall allowed bubbles greater movement and deformation. The unique regime transition will impact the IATE models for large diameter pipes.

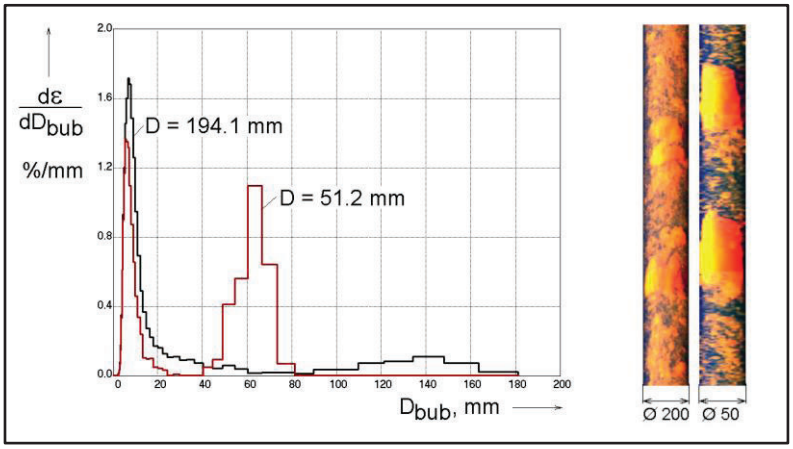

Figure 4: Comparison of bubble size distributions between a small and large diameter pipe for $j_g = 0.53\ m/s$ and $j_f = 1\ m/s$ [12].

3. RESULTS

In this section, key results will be presented in differing flow regimes. In the proceeding graphs, the discrete data represents experimental interfacial area concentration data from the TOPFLOW database, including error bars of ±10% error. A companion paper [13] addresses the error that is introduced by the algorithm required to determine interfacial area from void fraction data obtained from the wire mesh sensor. In the paper the error for spherical and Taylor bubbles remains below 5%. However, in order to account for additional uncertainty arising from estimation of bubble velocities, a conservative range of 10% is chosen.

The continuous data are results from TRACE-T, using the Fu and Ishii IATE formulation [11]. The color code is used to distinguish between different injection orifice sizes (red for 1 mm injection orifices, and blue for 4 mm injection orifices).

Two tests from the bubbly flow regimes are presented in Figure 5. TRACE-T performs fairly well for the 1 mm orifice injection, falling within or close to the 10% error bar range. The model performance for 4 mm injection in the bubbly regime is however not always consistent (poor for Test 6, good for Test 8). In general, good agreement is obtained at high liquid and low gas superficial velocities. However, the current model performance deteriorates significantly with increasing gas superficial velocity and decreasing liquid superficial velocities, as shown also in the results of Figure 6 (4 mm-orifices tests).

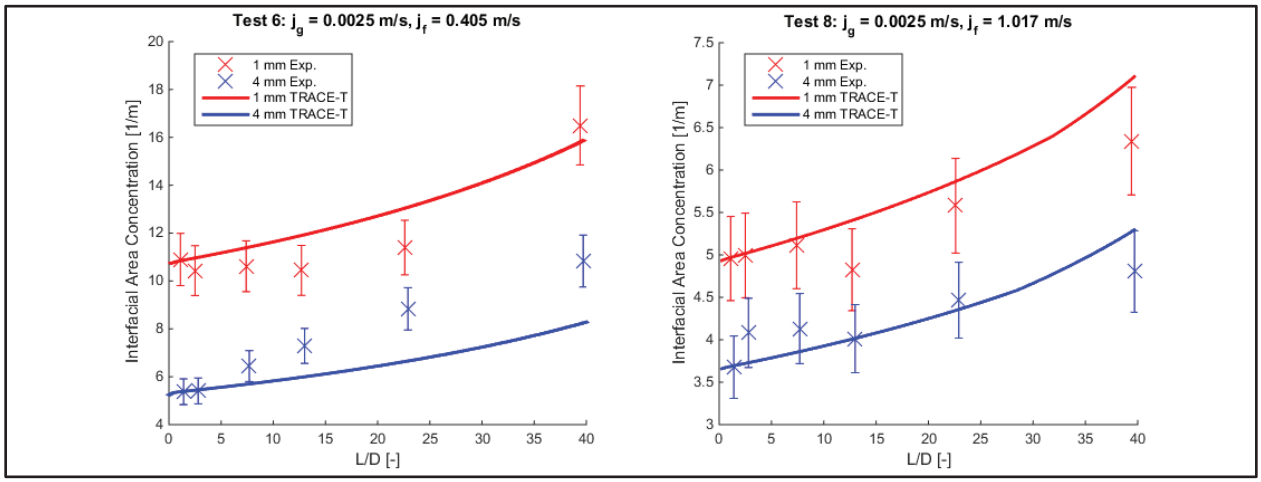

Figure 5: TRACE-T results for Test 6 (left) and Test 8 (right).

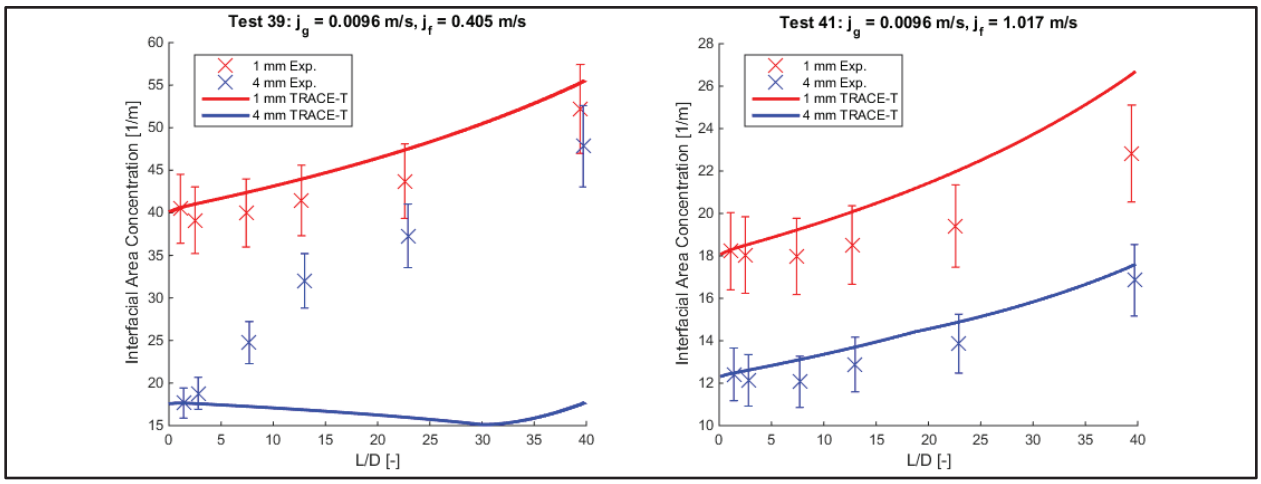

Figure 6: TRACE-T results for Test 39 (left) and Test 41 (right).

In order to understand the reasons for the discrepancies occurring at lower superficial liquid velocities, the predicted interfacial area source contributions along with the experimental void fraction distribution and bubble size histograms are analyzed. Figure 7 presents the source contributions for Test 39 and Test 41. Bubble expansion is the only dominant effect for the interfacial area propagation in Test 41, while all

other interactions have little impact. Bubble expansion is also prevalent in Test 39, however both wake entrainment and shearing off mechanisms are large contributors as well.

The fact that TRACE-T is underestimating the interfacial area for Test 39 (see Figure 6, left) is an indication that the model is over-predicting bubble coalescence, and under-estimating bubble break-up. Wake entrainment is the only coalescence mechanism contributing to the propagation which infers the coefficients for wake entrainment are incorrectly calibrated for a large diameter pipe. Past experiments may find greater incidence of the wake entrainment mechanism as small diameter pipes and bubbly flow at lower superficial liquid velocity are favorable to it. However, in a large pipe there is less confinement and greater movement available to the bubbles. This result indicates that the incidence of the wake entrainment mechanism in large diameter pipes is over-predicted. The possibility that, in addition, the shearing-off mechanism is underestimated will be discussed further in section 3.1.

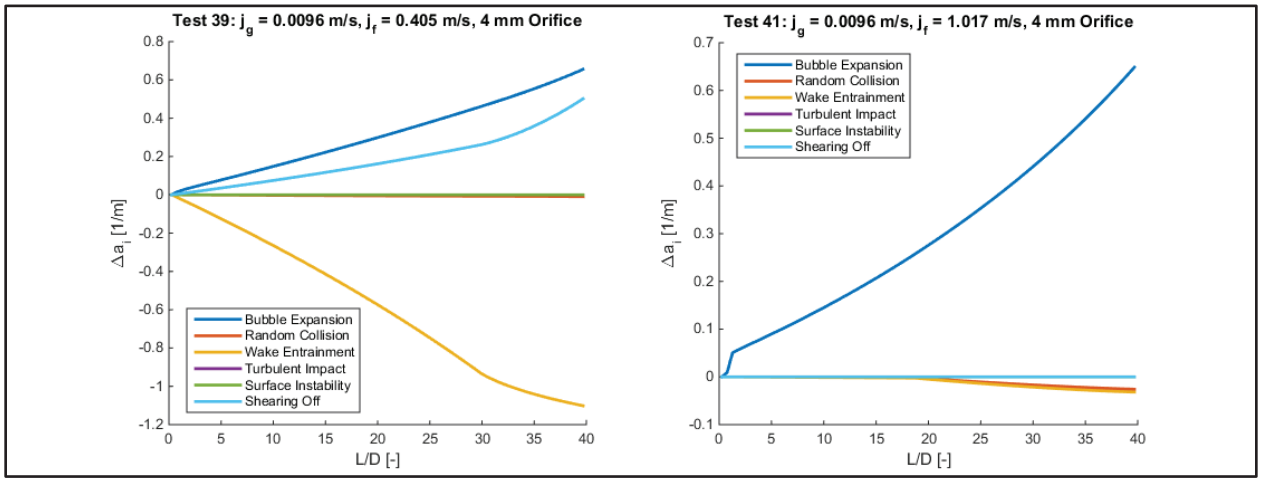

Figure 7: TRACE-T source contributions for Test 39 (left) and Test 41 (right).

The assertion that Test 39 (4 mm orifice injection) is break-up dominated is further supported by analyzing the void fraction distribution and bubble size histogram presented in Figure 8. The void fraction distributions indicate that the bubbles disperse throughout the flow cross-section, migrating from the pipe wall toward the center of the pipe, for increasing L/D from the injection location along the pipe axis. The bubble size distributions indicate that as the flow develops, the larger bubbles ($D > 15$ mm) undergo break-up resulting in a more prominent and narrow size distribution peaked at a diameter of about $D = 7.5$ mm.

It is interesting to note that for Test 41, for which good performance of the TRACE-T model is observed, the bubble size distribution remains mostly unchanged with increasing L/D (see Figure 9, right) confirming that the dominance of the sole bubble expansion effect is reasonable for this test. However, for decreasing liquid superficial velocity (Test 39), a significant bubble break-up is observed, as the bubble size distribution shifts toward lower diameters with increasing L/D (see Figure 8, right).

As mentioned in Section 2.1, the interaction mechanisms have coefficients that are determined empirically, with the exception of the bubble expansion mechanism, which is solely due to the pressure changes in the flow. These results further indicate that the coefficients that have been previously established require separate consideration for large diameter pipes.

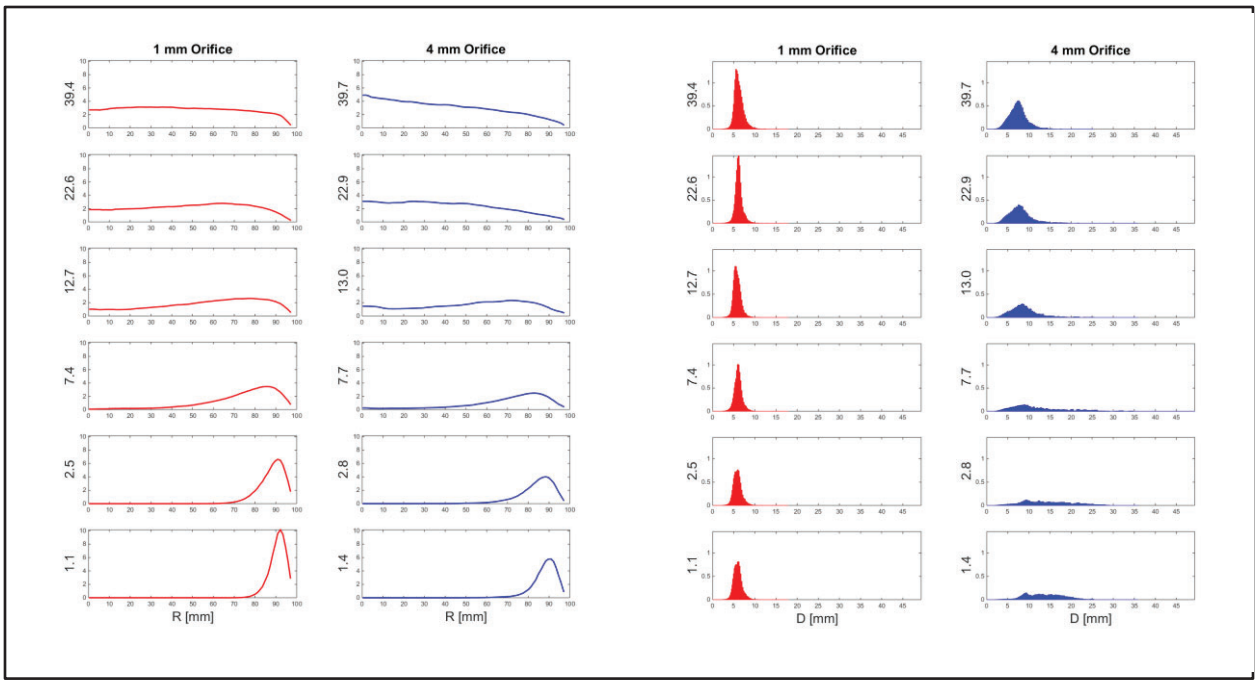

Figure 8: Experimental radial void fraction distribution (left) and bubble size histograms (right) for Test 39; the y-axis labels indicate L/D for the corresponding graph.

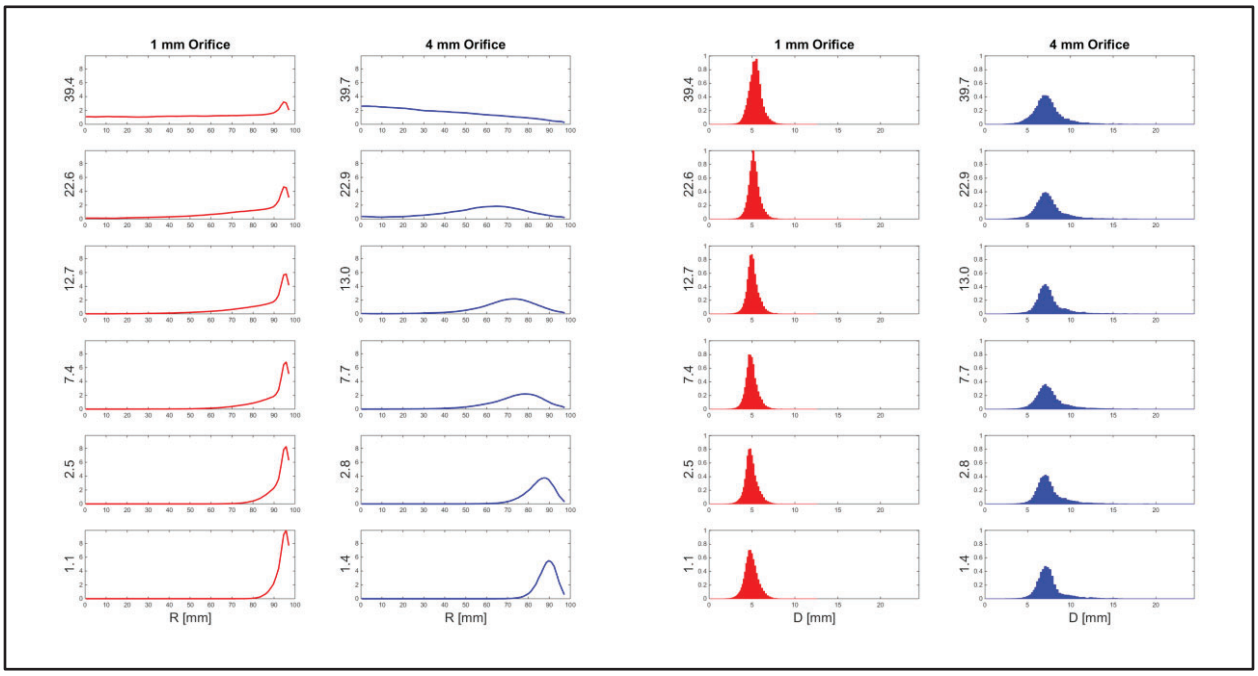

Figure 9: Experimental radial void fraction distribution (left) and bubble size histograms (right) for Test 41; the y-axis labels indicate L/D for the corresponding graph.

Results that have been discussed thus far have focused on the bubbly flow regime. Figure 10 presents results for Test 83 and Test 85, which are on the onset of the churn-turbulent flow regime. At the significantly higher superficial gas velocities, the experimental data indicates that the resulting interfacial

area is increasingly independent on the injection orifice size. TRACE-T performs poorly for all tests in the churn-turbulent regime (here we present only Test 83 and 85 for conciseness). Similar to Test 39 (4 mm orifice), the interfacial area is strongly under-predicted. Both the qualitative propagation of interfacial area and magnitude are incorrect. Figure 11 presents the source contributions as predicted by the model. Bubble expansion continues to play an important role, however, as discussed previously, this interfacial area source is expected to be accounted for appropriately.

Both Test 83 and Test 85 have two dominating interaction mechanisms, shearing off and wake entrainment. Reviewing the void fraction distribution and bubble size histograms, presented for Test 83 in Figure 12, will aid in determining which mechanisms dominated the flow. Both the void fraction distribution and bubble size distribution also appear to be independent of orifice size. The evolution of the bubble size histograms indicate that the initial large bubbles tend to break up and result in generation of a prominent peak at the low end of the bubble diameter spectrum. Again, this indicates that for large diameter pipe coalescence mechanisms such as wake entrainment are over-predicted and require reassessment.

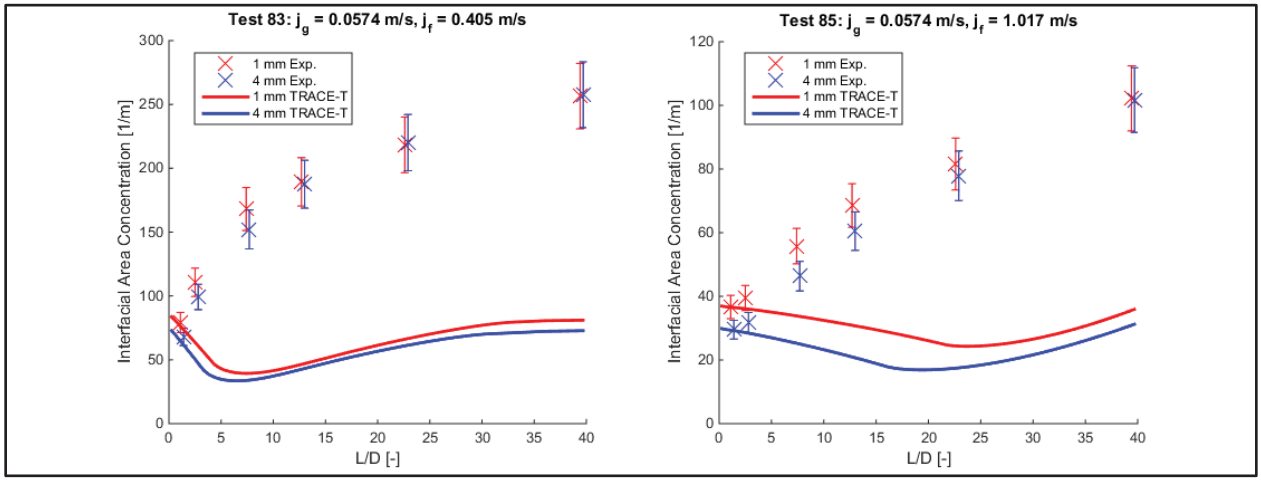

Figure 10: TRACE-T results for Test 83 (left) and Test 41 (right).

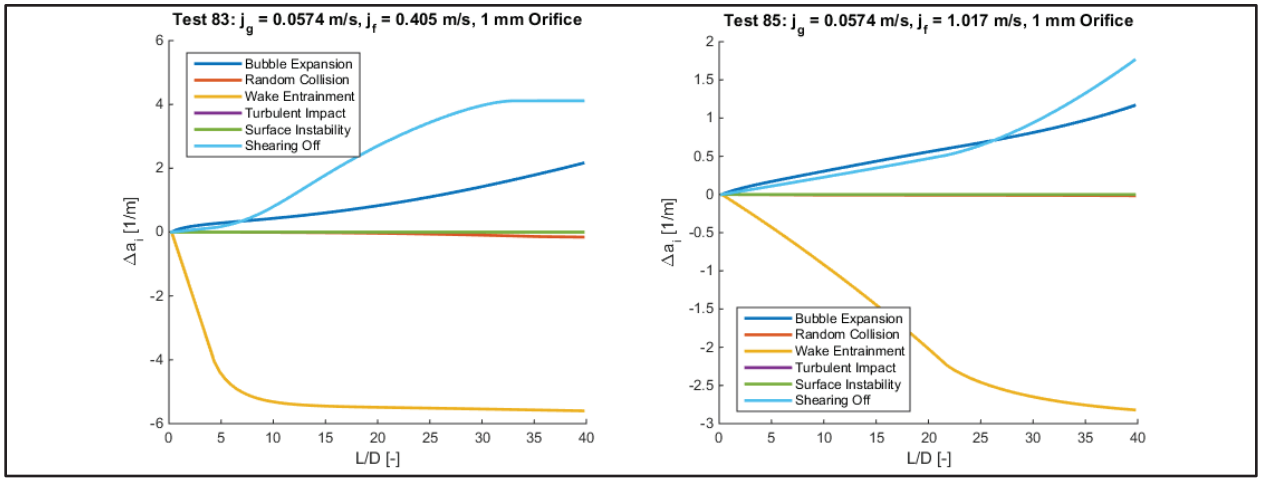

Figure 11: TRACE-T source contributions for Test 83 (left) and Test 85 (right).

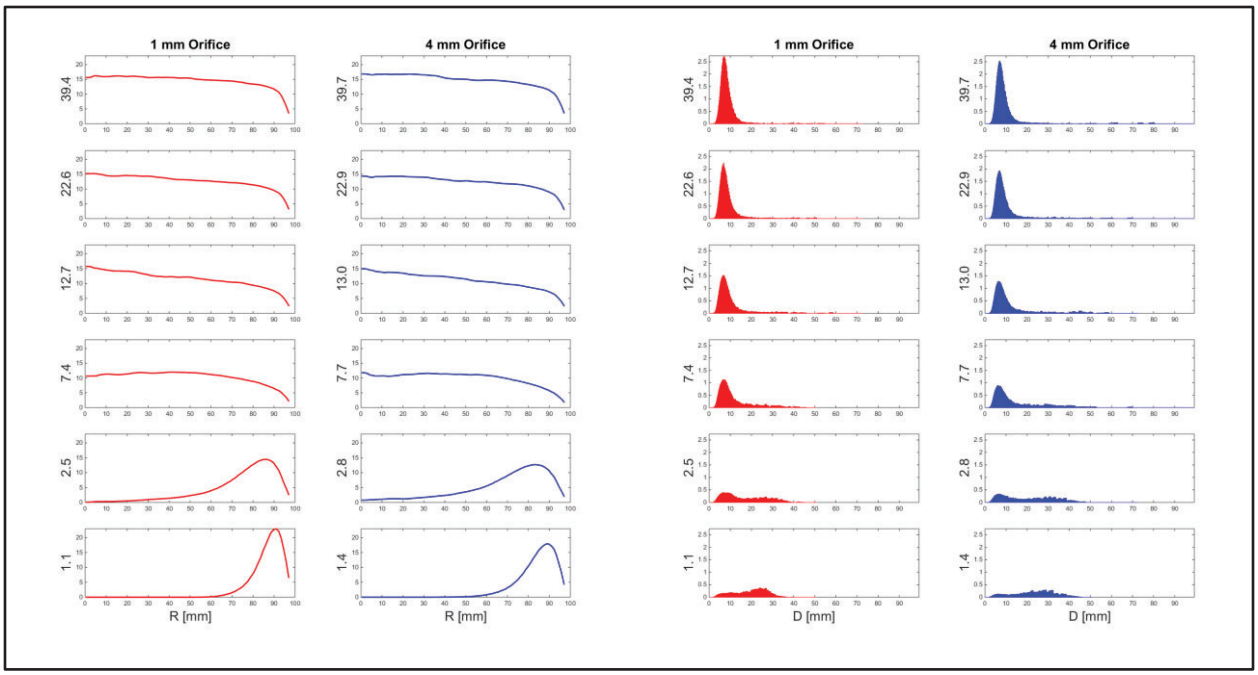

Figure 12: Experimental radial void fraction distribution (left) and bubble size histograms (right) for Test 83; the y-axis labels indicate L/D for the corresponding graph.

3.1 Sensitivity of two-group IATE model

Referring back to the discussion of Test 39 (4 mm orifice), it was concluded that the wake entrainment mechanism was overestimated. Figure 13 presents TRACE-T results when the wake entrainment mechanism is nullified. It is apparent that there is still a discrepancy between interfacial area prediction and experimental data.

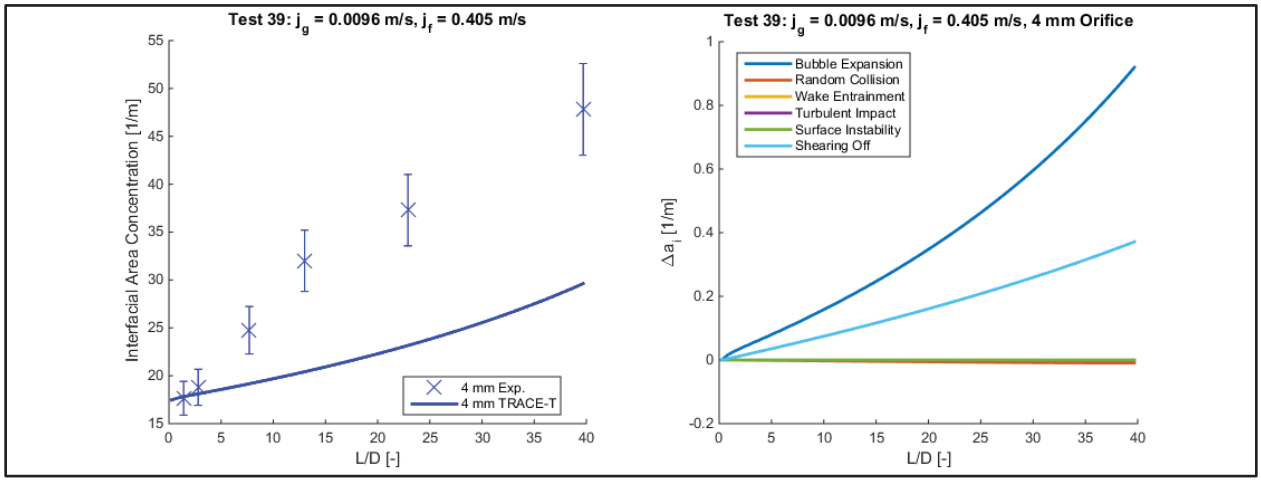

Figure 13: TRACE-T results (left) and source contributions (right) for Test 39 with wake entrainment coefficients nullified.

In order to further improve results for Test 39 (4 mm orifice) the shearing-off coefficient was increased to 8 times its original value of 0.03. The results are presented in Figure 14 (due to numerical instabilities experienced at $L/D > 25$, the results are truncated). Improvements in the magnitude and qualitative propagation of the interfacial area is promising. However, a comprehensive analyses of all available experimental data is still necessary.

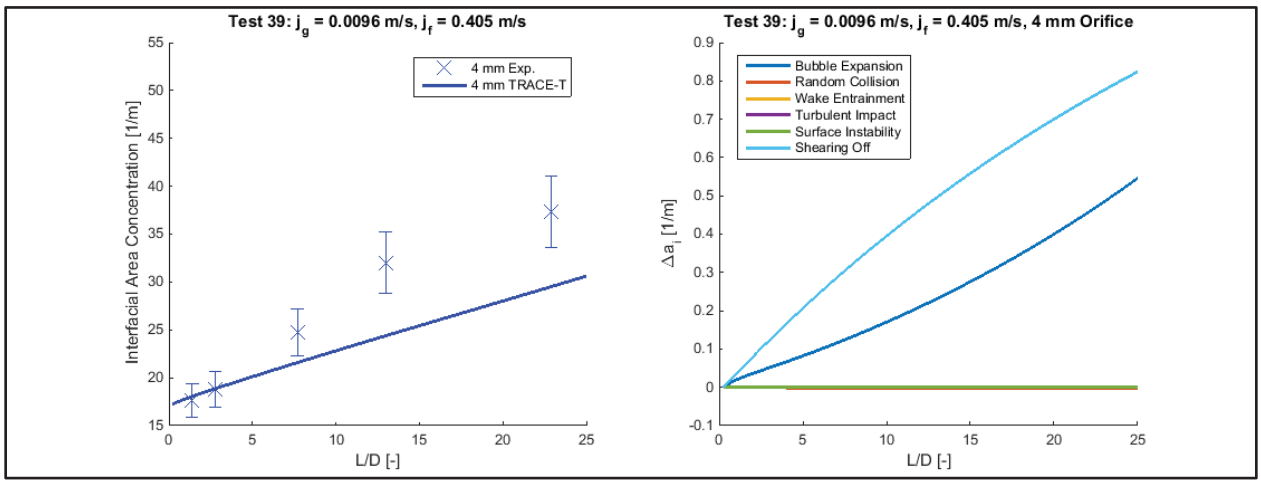

Figure 14: TRACE-T results (left) and source contributions (right) for Test 39 with Wake Entrainment coefficients nullified, 800% shearing off coefficient.

Test 83 also resulted in a large discrepancy in TRACE-T results (Figure 10). Figure 15 presents interfacial area propagation for TRACE-T when the wake entrainment coefficients are nullified and the shearing off coefficient is 500 times its original value (due to numerical instabilities experienced at $L/D > 14$, the results are truncated). Similar to the improvements realized for Test 39, the qualitative propagation and magnitude of interfacial area improves significantly. However, the shearing off coefficient required a significantly larger increase than that of Test 39. This can be interpreted as an indication that there might be additional break-up mechanisms currently not considered in the IATE model, and which become important in the churn-turbulent flows in large diameter pipe.

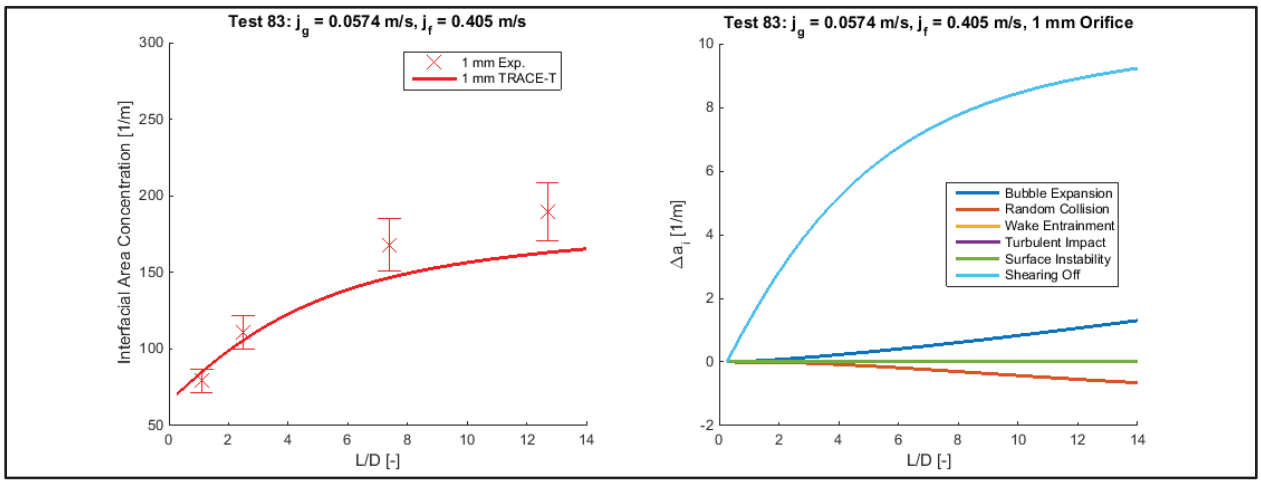

Figure 15: TRACE-T results (left) and source contributions (right) for Test 83 with wake entrainment coefficients nullified, 50,000% shearing off coefficient.

A recent paper by Liao and Lucas [14] reviewed models for bubble break-up processes. In addition to the three break-up processes presented in Figure 3, break-up can occur due to viscous shear forces. This mechanism occurs as viscous shear forces cause a local velocity gradient around the interface and deform the particle, leading to a break up. The velocity gradient can be instigated by turbulence or wake effect of other particles. This mechanism is not considered in the model implemented in TRACE-T and may play a significant role in large diameter pipes. However, literature supporting the phenomenological relations for viscous shear force break-up solely contains experiments that study simple shear flow. Further examination of experimental data is needed to determine average break-up time and frequency in vertical two phase flows for implementation in the two-group IATE model.

4. CONCLUSIONS

The study indicates that current mechanisms and coefficients for the two-group IATE model are not suitable for a majority of two-phase flow regimes in large diameter pipes. TRACE-T using the Fu and Ishii model performed fairly well (approximately 10% error) for bubbly flows with low superficial gas velocity and high liquid superficial velocities. The success in this low turbulence regime owed to the fact that bubble expansion (which solely depends on pressure drop, not empirical coefficients) was the driving mechanism for the interfacial area propagation. As the superficial gas velocity increases, the model incorrectly predicts that the wake entrainment mechanism has a large impact on the interfacial area propagation. Through the bubble size histograms obtained from the wire mesh sensor, it was evident that break-up mechanisms were dominating the flow development. While the wake entrainment mechanism may dominate the flow in a small diameter pipe where the wall confinement plays a major role, there is more freedom to disperse in a large diameter pipe. Also, the interaction between bubbles and large eddies in churn turbulent flows seems to not be well captured neither by the turbulent impact breakup model nor by the shearing off model.

Further considerations are needed to accommodate for the fact that the two-group IATE model may be lacking interaction mechanisms (such as break-up due to viscous shear forces) or under-estimating the importance of mechanisms that are more prominent in large diameter pipes.

NOMENCLATURE

Variable	Definition
a_{i1}	Group 1 interfacial area concentration
a_{i2}	Group 2 interfacial area concentration
α_1	Group 1 void fraction
α_2	Group 2 void fraction
v_{i1}	Group 1 interfacial velocity
v_{i2}	Group 2 interfacial velocity
v_{g1}	Group 1 gas velocity
v_{g2}	Group 2 gas velocity
η_{ph}	Volume introduced by phase change
C	Bubble shape distribution parameter
D_c	Critical bubble diameter
D_{sm1}	Group 1 Sauter-mean diameter
D_{sm2}	Group 2 Sauter-mean diameter
ϕ_{j1}	Group 1 interaction mechanisms

ϕ_{j2}	Group 2 interaction mechanisms
ϕ_{ph1}	Group 1 source/sink due to phase change

ACKNOWLEDGMENTS

The authors would like to acknowledge the TOPFLOW experimental team of the Helmholtz-Zentrum Dresden-Rossendorf. The work has been partially sponsored by the United States Nuclear Regulatory Commission, through grant No. NRC-HQ-60-14-G-0008.

REFERENCES

1. M. Beyer, D. Lucas, J. Kussin, P. Schütz, "Air-water experiments in a vertical DN200-pipe," *Forschungszentrum Dresden Rossendorf* (2008).
2. M. Ishii and S. Kim, "Development of One-group and Two-group Interfacial Area Transport Equation," *Nucl. Sci. Eng.* **146**(3), pp. 257-273 (2004).
3. J. Talley, "Interfacial area transport equation for vertical and horizontal bubbly flows and its application to the trace code," *Ph.D. Thesis, Pennsylvania State University* (2012).
4. M. Bernard, T. Worosz, S. Kim, C. Hoxie, S. Bajorek , "Comparison of Results in the Prediction of Cap/slug flows between Trace-T and Trace V5.0 Patch 3," *NURETH-15* (2013).
5. T.R. Smith, J. P. Schlegel, T. Hibiki, and M. Ishii, "Two-phase flow structure in large diameter pipes," *International Journal of Heat and Fluid Flow*, **33** (2012).
6. T.R. Smith, J. P. Schlegel, T. Hibiki, M. Ishii, "Mechanistic modeling of interfacial area transport in large diameter pipes," *International Journal of Multiphase Flow*, **47** (2012).
7. H.-M. Prasser, M. Misawa, I. Tseanu, "Comparison between wire-mesh sensor and ultra-fast X-ray tomograph for an air-water flow in a vertical pipe," *Flow Measurement and Instrumentation*, **16** (2005).
8. A, Manera, B. Ozar, S. Paranjape, M. Ishii, and H. Prasser, "Comparison between wire-mesh sensors and conductive needle-probes for measurements of two-phase flow parameters." *Nuclear Engineering and Design,* **239**, pp. 1718-1724 (2008).
9. T. Hibiki, M. Ishii, "Two-group Interfacial Area Transport Equations at Bubbly-to-slug Flow Transition," *Nuclear Engineering and Design,* **202**, pp. 39-76 (2000).
10. M. Ishii, T. Hibiki, "Thermo-fluid dynamics of two-phase flow 2nd Edition," *Springer*, New York (2010).
11. X. Y. Fu, M. Ishii, "Two-group Interfacial Area Transport in Vertical Air-water Flow I. Mechanistic Model", *Nuclear Engineering and Design*, **219**, pp. 143-168 (2002).
12. H.-M. Prasser, M. Beyer, A. Böttger, H. Carl, D. Lucas, A. Schaffrath, P. Schütz, F.-P. Weiss, J. Zchau, "Influence of the pipe diameter on the structure of the gas-liquid interface in a vertical two-phase flow," *NURETH-10* (2003).
13. A. Dave, A. Manera, M. Beyer, D. Lucas, H.-M. Prasser, "Uncertainty analysis of an Interfacial Area Reconstruction Algorithm," *NURETH-16* (2015).
14. Y. Liao, D. Lucas, "A literature review of theoretical models for drop and bubble breakup in turbulent dispersions," *Chemical Engineering Science*, **64**, pp. 3389-3406 (2009).